

numerous cutting-edge sciences. HES1 will be a general-purpose pump-probe experimental station, at which experiments related to the following fields [4–10] will be feasible, with various pump-probe techniques being facilitated by the fs optical laser pulse:

- Imaging of phonons in nano-particles;
- Examination of ultrafast dynamics in materials, e.g., under high magnetic fields;
- Investigation of ultrafast dynamics in chemistry, e.g., artificial photosynthesis and bond formation in solution;
- Examination of dynamic structural biology including protein dynamics.
- This article describes both the overall design and the critical components of HES1. This station setup was established in accordance with the following criteria:
- The beamline components have been designed to easily accommodate user-made instruments, in order to provide a variety of research opportunities;
- The optics have been designed with great care in order to preserve the XFEL wavefront;
- The two experimental end-stations in the hard x-ray beamline will have the same frontends. Common components will be shared and located at the frontend to yield improved efficiency.

This design report aims to provide information to facilitate the planning of experiments at HES1 and is organized as follows. Section 2 describes the hard x-ray optics design and the photon beam parameters, whereas Section 3 describes the beamline components and their layout. Finally, a summary and a future perspective are given in Section 4.

## 2. XFEL optics

The XFEL beam, which will have a photon flux of  $\sim 10^{12}$  per single pulse, a repetition rate of 60 Hz, and a pulse width of  $< 100$  fs, will be delivered through the beamline optics to support various experiments. The detailed specifications of the photon beam have been reported elsewhere [11]. Although the PAL-XFEL hard x-ray undulator will be capable of lasing a 2–20 keV XFEL beam, it would be impractical to optimize the end-station for the entire photon energy range with a single beamline component combination. In the first phase of the construction project in 2015,

beamline components such as the optics, vacuum windows, and attenuators will be prepared so as to yield the 5–12 keV photon energy range that is usually required for hard x-rays [12]. Realization of the 2–5 and 12–20 keV energy ranges is planned for the next phase of the project.

Three flat offset mirrors (M1, M2, and M3) and a double crystal monochromator (DCM) will be the main optical components in the hard x-ray beamline, which will be installed in the optics hutch (OH) shown in the beamline floor map given in Fig. 1(a). The XFEL beam will be delivered to the experimental areas through one of three paths in accordance with the optics arrangements, i.e., M1+M2, M1+M3, or DCM only. The colored dotted lines in Fig. 1(b) show the different beam trajectories. Regardless of the placement of the optics, the exit beam path will remain constant, although the exit beam properties will vary with the beam trajectories.

### 2.1. Flat offset mirror system

For diffraction experiments on non-crystalline systems, bio-samples, and other weak scattering objects, the maximum achievable photon flux at the sample position is a prerequisite for obtaining meaningful results. In these applications, a large bandwidth, even the natural XFEL bandwidth of 0.2% [13,14], is acceptable and no further bandwidth reduction is required. The photon-energy-dependent total external reflection property [15] will be used for rejection of the higher harmonic energies from the incident x-ray beam, with higher photon energy components being mostly absorbed. For the hard x-ray beamline, the double flat mirror system will be adopted for harmonic rejection. This will provide a fixed beam offset of 30 mm in the upper vertical direction and filter out the higher-order photon energy components of more than a few orders of magnitude. Low-pass filtering of the XFELs in a wide energy range of up to 20 keV will be implemented using combinations of the three mirrors, so as to allow selection of two energy regions (Fig. 1(b)): (1) M1+M2 for low energy (2–10.2 keV); (2) M1+M3 for high energy (10.2–20.1 keV). Detailed information on the mirrors is listed in Table 1.

### 2.2. Double Crystal Monochromator (DCM)

For various experimental applications such as diffraction and spectroscopy experiments, the energy bandwidth of the XFEL

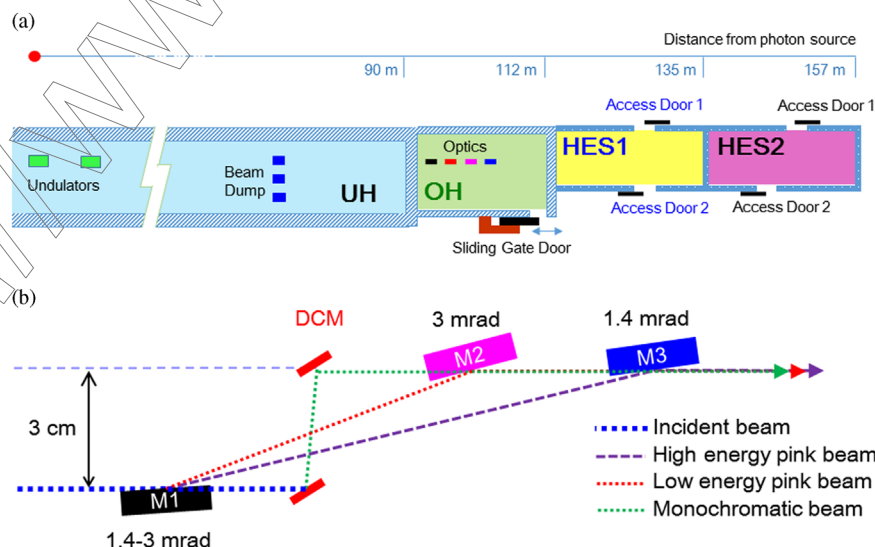


**Fig. 1.** (a) Floor map of hard x-ray beamline (top view). (b) Schematic diagram of optics in optics hutch (side view). UH: undulator hall, OH: optics hutch, DCM: double crystal monochromator.

should be narrower than the natural value. Reduction of the bandwidth requires the addition of a monochromator system. A monochromatic hard x-ray with an energy bandwidth,  $\Delta E/E < \sim 0.01\%$ , where  $E$  is the photon beam energy, will be delivered to the end-stations by a carefully designed DCM system. The DCM will be placed  $\sim 97$  m downstream of the photon source between offset mirrors M1 and M2 in the OH, as shown in Fig. 1(b). Si(111) single crystals, which are widely adopted for synchrotrons [16] and XFEL facilities [17], will be set as the primary monochromator crystals. This design is intended to deliver a full hard x-ray energy range of 2–20 keV, as the Bragg angles of the silicon crystals can vary from  $5.67^\circ$  to  $81.5^\circ$ .

A critical requirement of the DCM system is the provision of sufficient mechanical robustness to deliver fixed central XFEL beam energies. Weak mechanical stiffness results in long-term drift, and causes the delivered photon beam to have additional variations in photon energy, intensity, and position, regardless of the XFEL beam's innate jitter [18]. To minimize such additional variations, the DCM system is designed to have mechanical stability for a Bragg angle of less than  $0.3 \mu\text{rad}/15$  h, which corresponds to  $14.9 \text{ meV}/15$  h at 10 keV.

### 3. Design and components

#### 3.1. Overview of HES1

From a technical point of view, the instruments selected for use in HES1 are also prepared for experiments conducted in optical reflection geometry. Hence, the end-station in the first phase will

**Table 1**  
Offset mirror specifications.

Detail	Mirror		
	M1	M2	M3
Purpose	Higher harmonic rejection		
Type	Plane		
Distance from source (m)	94.7	99.7	105.4
Incident angle (mrad)	1.4 or 3	3	1.4
Direction	Upward	Downward	
Energy cut-off (keV)		10.2	20.4
Coating/Substrate	C/Si		
Substrate dimension (L × W × H, mm)	600 × 50 × 50		
Effective area (L × W, mm)	~580 × 20		

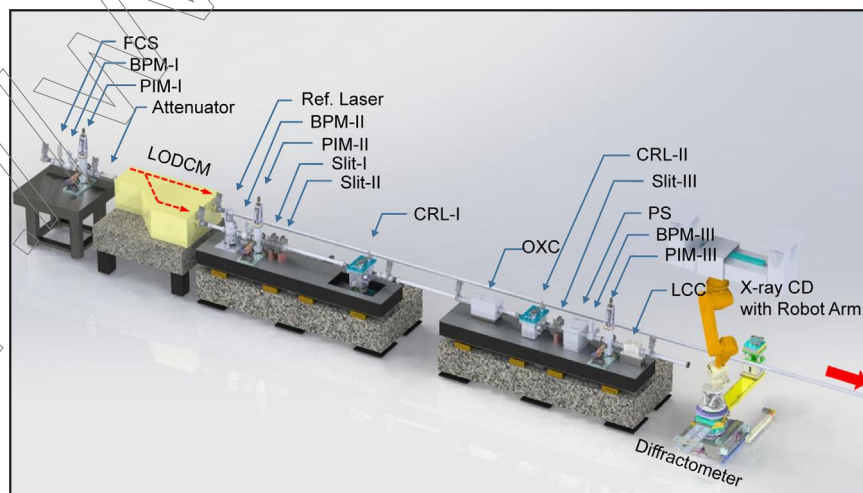
be built and specialized for pump and probe experiments such as Bragg coherent diffractive imaging (CDI) [6] and time resolved x-ray solution scattering (TRXSS) [19].

Fig. 2 shows a schematic view of the proposed HES1 components. All the components will be contained within an additional building inside the experimental hall, which is referred to as an experimental hutch, for protection from radiation exposure and to maintain a constant environmental temperature. A reference laser will be located behind the beam multiplexing system for efficient XFEL beam alignment. Photon-beam diagnostic apparatus such as the beam position monitor (BPM) and the profile intensity monitor (PIM) will be positioned so as to measure the beam position and intensity profile properties of the XFEL beam, respectively. The relative arrival time jitter between a given pump laser and the XFEL will be measured with an fs temporal resolution by an optical-laser and x-ray correlator (OXC). A pulse selector (PS), which is a fast XFEL beam shutter, will be installed to allow selection of the desired number of XFEL pulses. Two sets of Beryllium compound refractive lenses will be installed as focusing optics. To define and optimize the XFEL beam size, three slit sets will be available: two before and one after the focusing optics. A hexapod-equipped diffractometer will be located at the focal point of the focusing optics for sample positioning. At the end of the instrument array, a robotic detector arm will be installed for precise manipulation of the detectors. Detailed descriptions of the following important components are provided in this paper: the experimental hutch, diagnostics, XFEL beam multiplexing system, focusing optics, diffractometer, and robotic detector arm. Other critical components will be presented in separate reports.

#### 3.2. X-ray hutch

The XFEL experiments will be conducted in the experimental hutch, which contains a radiation-shielding hutch, beamline components, experimental instruments, and remote control systems. The HES1 hutch will be  $22 \text{ m} \times 8 \text{ m} \times 4.5 \text{ m}$  (length × width × height) and located  $\sim 113$  m downstream of the XFEL photon source. The environment in the hutch will be maintained at  $23 \pm 1^\circ \text{C}$ . The floor surface, which is already prepared, is coated with an epoxy resin paint and cast with 500-mm steel fiber reinforced concrete (SFRC) of 1500-mm thickness. The floor supports a load of  $3 \text{ t}/\text{m}^2$ . The flatness of the floor is controlled to within  $\pm 2 \text{ mm}$  over  $10 \text{ m}^2$ .

The XFEL beam height from the floor level will be fixed to 1430 mm over the full x-ray photon energy range. To prevent vibration, all experimental instruments will be installed on granite



**Fig. 2.** HES1 configuration. BPM: beam position monitor, PIM: profile intensity monitor, CRL: compound refractive lenses, OXC: optical-laser and x-ray correlator, PS: pulse selector, LCC: laser in-coupling chamber.

supports, and devices that cause vibrations (e.g., roughing pumps) will be installed on isolated supports. Any heat sources that could cause thermal instability (e.g., data servers) will be installed outside of the experimental hutch.

The final stage of the optical laser system will also be located in this hutch. The optical laser source will be installed on the second floor of HES2, and the path of the delivered optical laser will be combined with the XFEL beam path via a laser in-coupling chamber. An overhead crane (maximum lifting weight: 1 t; height: 4 m) will be located at HES1 to transport heavy items such as user-made sample chambers during installation.

### 3.3. XFEL photon beam diagnostics

A profile intensity monitor (PIM) is an offline instrument that measures the spatial profile, position, and intensity of the XFEL on a shot-by-shot basis. In this facility, the X-ray scintillation on a single-crystal YAG:Ce will be captured by an optical microscope, which will have an 8- $\mu\text{m}$  spatial resolution in a  $\sim 2\text{ mm} \times 2\text{ mm}$  field of view and the ability to be retracted from the beam path when the photon beam is delivered to the sample. To facilitate measurement of the shot-to-shot arrival time jitter between the optical laser and the XFEL, OXCs [20,21], which constitute a type of in-line diagnostic device, will be located at two points along the XFEL beam path. One of the OXCs will encode the jitter spectrally and the other spatially. They will provide sub-10-fs root mean square (RMS) resolutions by detecting x-ray-induced optical property changes in thin transparent membranes, for example, in  $\text{Si}_3\text{N}_4$ . A BPM, which is an in-line diagnostic recording device that can simultaneously measure the input photon flux and the spatial positions of the XFELs, will be included [22]. This tool functions by sensing x-ray photons back scattered from a highly transmissive thin membrane. Both the time tool and the BPM are in-line tools that operate on a shot-by-shot basis and in a non-invasive manner.

### 3.4. Optical laser system

In many cases, the pump and probe experiments will be performed with the ultrashort optical laser to investigate the time-resolved dynamics. The optical pulse can act as either a pump or a probe. Regardless of its role, the optical laser should be able to stimulate or characterize the sample with appropriate photon energy or optical wavelength. The end-stations will provide an ultrashort laser pulse that will be tunable over a wide spectral range.

Fundamental tens-of-fs pulses at 800 nm can be delivered from the Ti:Sapphire regenerative amplifier system, which will be synchronized to the master radio frequency (RF) and the event timing system. It will be possible to change the repetition rate to an integer division of 120 Hz, depending on the experimental scheme in question. The optical parametric amplifier will extend the spectral tunability of the system from the ultraviolet (UV, e.g., 240 nm) to the mid-infrared (IR, e.g., 20  $\mu\text{m}$ ) regions. This widely tunable spectral range will provide the optimal optical pulse to stimulate or characterize a sample.

### 3.5. Beam-multiplexing system: large-offset double crystal monochromator

Since only a single experiment can be performed in one end-station at a time during operation of an x-ray beamline at the XFEL facility, quite limited user beam time and extremely high operation costs are expected. In order to alleviate this economics related issue and to improve the efficiency of use of the XFEL, simultaneous operation of the two tandem end-stations, HES1 and HES2, is planned. Thus, the beam will be divided and shared between the

stations using a thin single crystal [23]. The beam-sharing concept shall be realized using an XFEL beam multiplexing system, in particular, a large-offset double crystal monochromator (LODCM) [24,25] located 115 m from the photon source. The LODCM is designed to split a single incident XFEL beam into two parallel beams with a 600-mm offset. Since all the beamline components of the HES1 instrument can be translated and placed at their beam offset positions, simultaneous operations in the two branch beamlines, HES1 and HES2, can be achieved. Note that this multiple-branch operation apparatus will be implemented in the near future, as the engineering techniques involved in the LODCM require additional development time.

### 3.6. Focusing optics: beryllium compound refractive lenses

Since the photon flux density is directly related to decreases in the signal intensity over the propagation distance, it is essential to use focusing optics to take full advantage of the XFELs. Beryllium compound refractive lenses (CRLs) will be used for beam focusing at this end-station, because they are sufficiently robust to withstand the full XFEL beam and can provide the desired photon flux density gain. Two sets of CRLs, having short ( $f=3.6\text{ m}$ ) and long ( $f=7.2\text{ m}$ ) focuses, will be located 125.4 and 121.8 m downstream of the XFEL photon source, respectively. Each set will contain 8 stacks of CRLs to focus the XFELs from 5 to 12 keV in 1-keV increments. Every lens stack in the long focus set will deliver the desired focal spots (full width at half maximum (FWHM))  $\sim 10\text{ }\mu\text{m}$  [12], while the stacks in the short focus set will yield tighter focal spots (FWHM  $\sim 5\text{ }\mu\text{m}$ ); note that the focal spot size is proportional to the magnification factor [26]. The focal spots formed by those two sets will coincide at the sample position, which is located 129 m from the photon source to facilitate easy sample alignment. The designed transmittances of the lens stacks are more than  $\sim 50\%$  at minimum.

### 3.7. Pulse selector

The fundamental repetition rate of PAL-XFEL will be 60 Hz, corresponding to a pulse period of  $\sim 16.7\text{ ms}$ . In some experiments, however, only certain pulses must be transmitted and all others must be blocked for various reasons. For example, a sample-destructive, fixed-object experiment may be difficult to perform with the above pulse period, because the required sample alignments on the XFEL beam path could not be accomplished within this time scale.

A PS can be used to overcome this issue. This device permits only the desired selected pulses to pass, and is essentially an electrically controlled optical switch. The PS will reduce the repetition rate of the pulse to an integer division of the fundamental repetition rate. It will enable only a single pulse to interact with the sample and will protect the samples from radiation damage. This device can also function in burst picker mode, which can be applied in order to select a certain pulse train pattern. In this mode, only a user-defined number of XFEL pulses will be transmitted for interaction with the sample.

Piezo-motor-driven tungsten teeth, such as those shown in Fig. 3, will be used to block  $\sim 100\%$  of the XFEL beam intensity within a switching time of  $< 3\text{ ms}$ , and with a close/open cycle time of 8 ms. This will yield the full PAL-XFEL flux over the full photon energy range of 2–20 keV, without disturbance of the XFELs. A tungsten-based, teeth-structured optical head provides low transmission and durability against high photon flux. It can withstand a full photon flux with a maximum of 1.0 mJ per pulse, and the transmission through the blade is  $< 10^{-11}$  over the full photon energy range. The clear aperture will be  $> 3\text{ mm}$  ( $6\cdot\sigma$ ) which is larger than the beam size over the full spectral range at the PS location. When the control

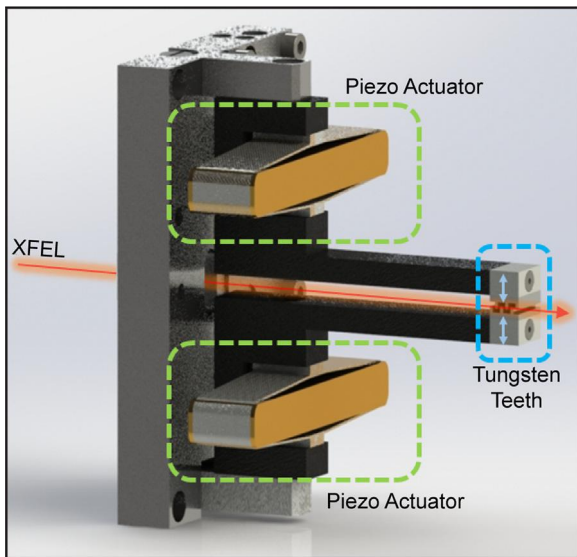


Fig. 3. Piezo-driven x-ray pulse selector.

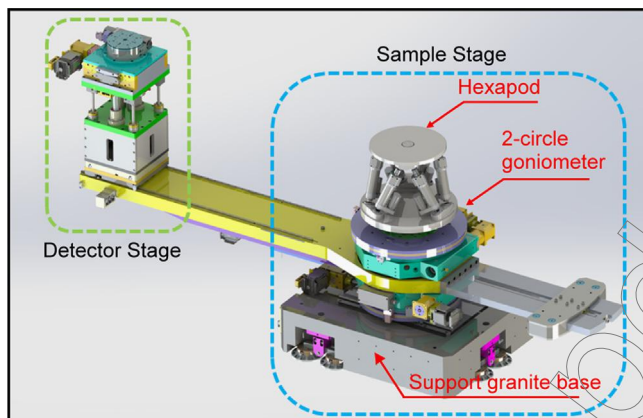


Fig. 4. 3D diagram of diffractometer system.

voltage is applied, the PS will open a clear aperture with dimensions of  $3\text{ mm} \times 5\text{ mm}$ . The selector will typically be closed, and will be driven by a standard electronic board delivering a transistor logic (TTL) signal of  $-20$  or  $150\text{ V}$ .

### 3.8. Diffractometer

A diffractometer system, as shown in Fig. 4, will be located at the end of HES1, at a distance of  $129\text{ m}$  from the photon source. This will allow the positions and orientations of the samples and detectors to be precisely adjusted in relation to the XFEL beam path. The diffractometer system will comprise an assembly of two mechanical sub-components: sample and detector stages. Heavy experimental instruments will be allowed so as to facilitate diverse experiments: up to  $290\text{ kg}$  for the sample stage and up to  $100\text{ kg}$  for the detector stage.

The sample stage will be composed of a 2-circle goniometer and a hexapod. The goniometer will drive independent rotations of the sample and detector stages horizontally. The entire sample stage will be mounted on a supporting granite base. The sample chambers will be loaded and fixed on the top platform of the hexapod, which will allow adjustable positioning of the chambers along three tilting and three translational axes. The detector stage will be a positioning device for a secondary detector while a robot arm, which will be discussed in the next chapter, will be used for

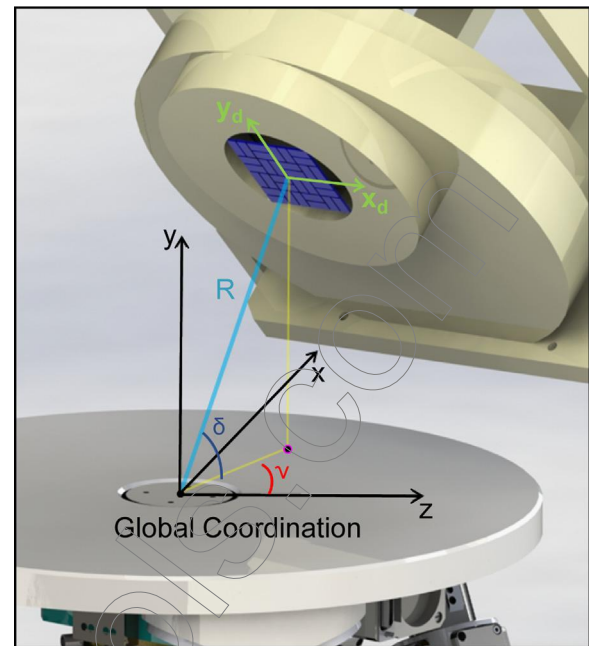


Fig. 5. Global coordination system with XFEL beam propagating along z-axis.  $R$ : radial distance,  $\nu$ : azimuth angle,  $\delta$ : altitude angle, where the zenith direction is along the y-axis,  $x_d$  and  $y_d$ : pixel coordinates on the detector plane.

Table 2

Robot arm detector coverage.  $\nu$  is the azimuth angle,  $\delta$  is the altitude angle, and  $R$  is the radial distance, where the zenith direction is along the y-axis.

	Forward	Backward
$\nu$	$-15\text{--}105^\circ$	$105\text{--}180^\circ$
$\delta$	$-15\text{--}90^\circ$	$-15\text{--}90^\circ$
$R$	$10\text{--}100\text{ cm}$	$10\text{--}50\text{ cm}$

the primary detector. Users can adjust the sample-to-detector distance from  $0.5$  to  $1.5\text{ m}$  using a manual linear translator.

### 3.9. Robotic detector arm

Two-dimensional aerial detectors are widely adopted in various application fields involving either synchrotron or XFEL facilities, because of their advanced performance. A pixelated aerial detector will be the main data recording instrument in HES1, and detailed specifications of this device can be found elsewhere [27]. Since the recently developed detectors for XFEL photon sources tend to be heavier than  $20\text{ kg}$ , a robotic detector arm is a suitable machine to manipulate such a heavy module with pixel accuracy.

HES1 will adopt a high-precision medium-payload robot arm [28] with six degrees of freedom for accurate positioning within the spatial coverage. The robotic detector arm will enable users to trace any point in the reciprocal space over the entire coverage and will always orient the 2D detector surface to a tangential plane centered on the interaction point. Referring to the coordination system defined in Fig. 5, forward and backward scattering geometries with regards to the detector position will be permitted. Table 2 shows the detector coverage.

### 3.10. Four-way slits

To exploit the full performance of the PAL-XFEL, the instruments must deliver every useful photon from the XFEL beam so as to maximize the signal-to-noise ratio of the detected signal. Slits are required to define the x-ray beam for the end-station. The x-ray beam size will be varied in accordance with the requirements of the various experiments, so an adjustable aperture is essential. Three slits will be positioned in order to accommodate different scenarios. Slits I and II will define the main beam before the focusing optics for energies over and below 7 keV, respectively, while slit III will eliminate the parasitic scattering after the focusing optics.

The PAL-XFEL beam is expected to have a sharp Gaussian profile enveloped in spontaneous radiation and parasitic noise from the optics. Four-way slits will be adopted to reject those off-axis noises without affecting the XFEL beam. The most x-ray-absorbent materials that are also robust to the beam will therefore be selected, and each slit will consist of four independently moving blades. The materials to be used in the blades will be selected based on the photon energy range. In addition, elaborately polished blades (polished to a roughness of  $< 25$  nm RMS) will be used to minimize parasitic scattering, with a transmission of  $\leq 10^{-20}$  over the entire 2–20-keV energy range. A heavy material is needed to reject third-harmonic radiation, but the reduced intensity of the third harmonics compared with the fundamental radiation will allow heavy materials to be used without damage. For energies  $< 7$  keV, the blades will be composed of  $\text{Si}_3\text{N}_4$ , but for energies  $> 7$  keV  $\text{Ta}_{90}\text{W}_{10}$  alloy plate will be used, because this heavy material can attenuate the third harmonics sufficiently. The positioning accuracy and repeatability of the blade manipulators will be within  $\pm 2$   $\mu\text{m}$ . The aperture size will be up to 30 mm  $\times$  30 mm when fully opened, and the blades will be overlapped when closed.

### 3.11. Sample environment

Samples are required to be isolated in specific environments in accordance with the purposes of the various experiments. HES1 will have multi-purpose sample chambers to support such experimental conditions. However, users can bring their own sample chambers to accommodate their particular requirements. In this case, the chamber weight should be less than 290 kg, which is the maximal payload of the diffractometer, to yield the desired sample environments. It is recommended that all sample chambers be equipped with a long-distance video microscope as a viewing system. This is a useful tool for alignment of the XFEL, optical laser spots, and samples. General guidelines for sample chamber designs are given below.

- The chamber should be compatible with the built-in components:
  - Economy should be considered to be the first priority, because of the low XFEL beam time availability. Thus, the chamber design should exhibit machine stability and beam alignment efficiency;
  - Any materials loaded on the diffractometer system should not prevent the diffractometer and robot arm from operating;
  - The center of mass of the loads should be below the beam/rotation center of the diffractometer for safety and mechanical stability considerations;
  - It is recommended that all devices and peripherals in the chamber be designed so that it is possible to import them to the PAL-XFEL general control and data acquisition (DAQ) system. Otherwise, a dedicated control and DAQ system should be prepared.

## 4. Conclusion

HES1 is one of the two experimental end-stations that will be positioned at the hard x-ray beamline of PAL-XFEL. This end-station will provide built-in instruments, such as x-ray optics, photon diagnostic systems, an optical laser system, focusing lenses, a diffractometer, and a detector system. Intense, coherent, and short (only tens-of-fs) XFEL pulses will be delivered to the end-stations by the flat mirrors and DCM. Two combinations of the three flat mirrors in the optics hutch will be available, which will transport an incoming beam and filter the unwanted third harmonics. The DCM will deliver XFELs with a bandwidth of less than  $10^{-4}$ .

The characteristics of each individual XFEL pulse, including the intensity, profile, spatial position, and the arrival time will be monitored and recorded by in-line and off-line diagnostics at the front of the end-station. Two sets of CRLs will deliver focused XFEL pulses to the sample position in the 5–12 keV x-ray photon energy range. While a multi-purpose sample chamber will be prepared, user-made chambers with instruments (up to 290 kg) may also be loaded via the diffractometer system for maximal versatility. Since recently developed 2D detector systems for XFELs are more complex and larger than past designs, an accurate and stable manipulation system is crucial. A robotic detector arm will be equipped as a positioning device for the detectors, because of its satisfactory accuracy and stability.

HES1 will begin user service in early 2017 after one year of commissioning, which will be conducted in 2016. It will support various pump-probe experiments based on x-ray experimental techniques such as Bragg CDI, x-ray correlation spectroscopy, and coherent x-ray scattering.

## Acknowledgment

This material is based on work supported by the Ministry of Science, ICT, and Future Planning (MSIP) through the PAL-XFEL project, and by the Korean National Research Foundation (NRF) through the SRC (Grant no. NRF-2015R1A5A1009962). We thank Dr. Yong Woon Park for useful discussions on the photon beam properties of PAL-XFEL and Mr. Seokjung Kang for nice artwork.

## References

- [1] M. Ree, et al., *Synchrotron Radiat. News* 22 (5) (2009) 4.
- [2] S.H. Nam, et al., *Synchrotron Radiat. News* 26 (4) (2013) 24.
- [3] Y.W. Parc, et al., *J. Korean Phys. Soc.* 64 (7) (2014) 976.
- [4] K.H. Kim, et al., *Nature* 518 (7539) (2015) 385.
- [5] J. Yano, V. Yachandra, *Chem. Rev.* 114 (8) (2014) 4175.
- [6] J.N. Clark, et al., *Science* 341 (6141) (2013) 56.
- [7] M. Levantino, et al., *Nat. Commun.* 6 (6772) (2015), <http://dx.doi.org/10.1038/ncomms7772>.
- [8] E. Szilagy, et al., *Nat. Commun.* 6 (6577) (2015), <http://dx.doi.org/10.1038/ncomms7577>.
- [9] J. Tenboer, et al., *Science* 346 (6214) (2014) 1242.
- [10] W. Helml, et al., *Nat. Photon* 8 (12) (2014) 950.
- [11] Y.W. Parc, et al., *Nucl. Instruments Methods Phys. Res. Sect. A* 782 (2015) 120.
- [12] The 2nd XFEL Workshop on Dynamics, POSCO International Center, Pohang, Republic of Korea, Jan. 13–14, 2014.
- [13] T. Ishikawa, et al., *Nat. Photon* 6 (8) (2012) 540.
- [14] B. Sébastien, J.W. Garth, *New J. Phys.* 12 (3) (2010) 035024.
- [15] J. Als-Nielsen, D. McMorrow, *Elements of Modern X-ray Physics*, John Wiley & Sons, New York, 2011.
- [16] O.H. Seeck, *X-Ray Diffr.: Mod. Exp. Tech.* (2015) 29.
- [17] M. Yabashi, T. Ishikawa, XFEL/Spring-8 Beamline Technical Design Report Ver. 2.0. RIKEN/JASRI, 2010.
- [18] K. Tono, et al., *New J. Phys.* 15 (2013) 083035.
- [19] M. Cammarata, et al., *Nat. Methods* 5 (10) (2008) 881.
- [20] N. Hartmann, et al., *Nat. Photon* 8 (2014) 706.
- [21] M. Harmand, et al., *Nat. Photon* 7 (3) (2013) 215.
- [22] Y. Feng, et al., *Int. Soc. Opt. Photon.* 8140 (2011) 81400Q.
- [23] J. Als-Nielsen, et al., *Nucl. Instruments Methods Phys. Res. Sect. B* 94 (3) (1994) 306.
- [24] D. Zhu, et al., *Rev. Sci. Instruments* 85 (6) (2014) 063106.



ELSEVIER

Contents lists available at ScienceDirect

# Nuclear Instruments and Methods in Physics Research A

journal homepage: [www.elsevier.com/locate/nima](http://www.elsevier.com/locate/nima)

## Design of a hard X-ray beamline and end-station for pump and probe experiments at Pohang Accelerator Laboratory X-ray Free Electron Laser facility



Jaeku Park<sup>a</sup>, Intae Eom<sup>a</sup>, Tai-Hee Kang<sup>a</sup>, Seungyu Rah<sup>a</sup>, Ki Hyun Nam<sup>a</sup>, Jaehyun Park<sup>a</sup>, Sangsoo Kim<sup>a</sup>, Soonam Kwon<sup>a</sup>, Sang Han Park<sup>a</sup>, Kyung Sook Kim<sup>a</sup>, Hyojung Hyun<sup>a</sup>, Seung Nam Kim<sup>a</sup>, Eun Hee Lee<sup>a</sup>, Hocheol Shin<sup>a</sup>, Seonghan Kim<sup>a</sup>, Myong-jin Kim<sup>a</sup>, Hyun-Joon Shin<sup>a</sup>, Docheon Ahn<sup>a</sup>, Jun Lim<sup>a</sup>, Chung-Jong Yu<sup>a</sup>, Changyong Song<sup>b</sup>, Hyunjung Kim<sup>c</sup>, Do Young Noh<sup>d</sup>, Heung Sik Kang<sup>a</sup>, Bongsoo Kim<sup>a</sup>, Kwang-Woo Kim<sup>a</sup>, In Soo Ko<sup>a</sup>, Moo-Hyun Cho<sup>a</sup>, Sunam Kim<sup>a,\*</sup>

<sup>a</sup> Pohang Accelerator Laboratory, Jigokro-127-beongil, Nam-gu, Pohang, Gyeongbuk 790-834, Republic of Korea

<sup>b</sup> Department of Physics, POSTECH, 77 Cheongam-Ro, Nam-Gu, Pohang, Gyeongbuk 790-784, Republic of Korea

<sup>c</sup> Department of Physics, Sogang University, 35, Baekbeom-ro Mapo-gu, Seoul 121-742, Republic of Korea

<sup>d</sup> Department of Physics and Photon Science, GIST, 123 Cheomdangwagi-ro, Buk-gu, Gwangju 500-712, Republic of Korea

### ARTICLE INFO

#### Article history:

Received 17 July 2015

Accepted 24 November 2015

Available online 10 December 2015

#### Keywords:

X-ray free electron laser

Hard x-ray pump and probe

XFEL beamline

Time-resolved coherent x-ray scattering

Ultra-fast dynamics

PAL-XFEL

### ABSTRACT

The Pohang Accelerator Laboratory X-ray Free Electron Laser project, a new worldwide-user facility to deliver ultrashort, laser-like x-ray photon pulses, will begin user operation in 2017 after one year of commissioning. Initially, it will provide two beamlines for hard and soft x-rays, respectively, and two experimental end-stations for the hard x-ray beamline will be constructed by the end of 2015. This article introduces one of the two hard x-ray end-stations, which is for hard x-ray pump-probe experiments, and primarily outlines the overall design of this end-station and its critical components. The content of this article will provide useful guidelines for the planning of experiments conducted at the new facility.

© 2015 Elsevier B.V. All rights reserved.

### 1. Introduction

The Pohang Accelerator Laboratory X-ray Free Electron Laser (PAL- XFEL) is a new facility at the Pohang Accelerator Laboratory that will provide ultrashort x-ray laser pulses based on a self-amplified spontaneous emission (SASE) process. Overviews of the PAL-XFEL project have been given previously [1–3], and this facility will begin user operation in early 2017 following one year of commissioning in 2016. Then, fully coherent, bright, tens-of-femtosecond (fs) x-ray pulses will be delivered for experiments in various research areas.

In 2015, one hard and one soft x-ray beamline will be built initially, although the PAL-XFEL is ultimately planned to have three hard and two soft x-ray beamlines. The first hard x-ray end-station (HES1, tentatively) will be attached to the hard x-ray beamline for x-ray pump-probe experiments (XPP), and will be followed in tandem by the second hard x-ray experimental end-station (HES2, also tentatively), for coherent x-ray imaging (CXI) and serial femtosecond crystallography (SFX). HES1 will support various pump and probe experiments, in which optical laser pulses usually play a role as external triggers with XFEL pulses functioning as a probe. However, these roles may also be reversed. This unique facility is expected to contribute to the advancement of new eras in

\* Corresponding author. Tel.: +82 54 279 1558.

E-mail addresses: [pjaeku@postech.ac.kr](mailto:pjaeku@postech.ac.kr) (J. Park), [neplus@postech.ac.kr](mailto:neplus@postech.ac.kr) (I. Eom), [thkang@postech.ac.kr](mailto:thkang@postech.ac.kr) (T.-H. Kang), [syrah@postech.ac.kr](mailto:syrah@postech.ac.kr) (S. Rah), [structure@postech.ac.kr](mailto:structure@postech.ac.kr) (K.H. Nam), [fermi13@postech.ac.kr](mailto:fermi13@postech.ac.kr) (J. Park), [sangsookim@postech.ac.kr](mailto:sangsookim@postech.ac.kr) (S. Kim), [snkwon@postech.ac.kr](mailto:snkwon@postech.ac.kr) (S. Kwon), [sh0912@postech.ac.kr](mailto:sh0912@postech.ac.kr) (S.H. Park), [kyungkim@postech.ac.kr](mailto:kyungkim@postech.ac.kr) (K.S. Kim), [hjhyun@postech.ac.kr](mailto:hjhyun@postech.ac.kr) (H. Hyun), [ksn@postech.ac.kr](mailto:ksn@postech.ac.kr) (S.N. Kim), [leh@postech.ac.kr](mailto:leh@postech.ac.kr) (E.H. Lee), [striater@postech.ac.kr](mailto:striater@postech.ac.kr) (H. Shin), [kimsh80@postech.ac.kr](mailto:kimsh80@postech.ac.kr) (S. Kim), [mjk@postech.ac.kr](mailto:mjk@postech.ac.kr) (M.-j. Kim), [shj001@postech.ac.kr](mailto:shj001@postech.ac.kr) (H.-J. Shin), [adc4055@postech.ac.kr](mailto:adc4055@postech.ac.kr) (D. Ahn), [limjun@postech.ac.kr](mailto:limjun@postech.ac.kr) (J. Lim), [cju@postech.ac.kr](mailto:cju@postech.ac.kr) (C.-J. Yu), [cysong@postech.ac.kr](mailto:cysong@postech.ac.kr) (C. Song), [hkim@sogang.ac.kr](mailto:hkim@sogang.ac.kr) (H. Kim), [dynoh@gist.ac.kr](mailto:dynoh@gist.ac.kr) (D.Y. Noh), [hskang@postech.ac.kr](mailto:hskang@postech.ac.kr) (H.S. Kang), [kbs007@postech.ac.kr](mailto:kbs007@postech.ac.kr) (B. Kim), [xraykim@postech.ac.kr](mailto:xraykim@postech.ac.kr) (K.-W. Kim), [isko@postech.ac.kr](mailto:isko@postech.ac.kr) (I.S. Ko), [mhcho@postech.ac.kr](mailto:mhcho@postech.ac.kr) (M.-H. Cho), [ksn7605@postech.ac.kr](mailto:ksn7605@postech.ac.kr) (S. Kim).